

PACS numbers: 32.80.Bx; 42.50.Gy
DOI: 10.1070/QE2005v035n08ABEH003411

Numerical simulation of the quasi-resonance regime of a transient double resonance in a scheme with a common upper level at a large inhomogeneous broadening of quantum transitions

A.E. Dmitriev, O.M. Parshkov

***Abstract*. The transient double resonance in the Λ scheme is numerically investigated in the case of a strong inhomogeneous spectral broadening of a medium and nonzero detunings of the frequencies of interacting pulses from the central frequencies of corresponding quantum transitions. It is shown that the signal pulse efficiently interacts with the pump pulse only when a certain condition imposed on the nonzero detunings is satisfied. If this condition is strongly violated at the input to the resonance medium, only a weak field of the rear edge of the input signal pulse mainly interacts with the pump field. In this case, two pulses with different frequencies are formed in the signal channel. This is explained by the specific interaction of radiation with Doppler-broadened quantum transitions.**

Keywords: *transient double resonance, inhomogeneous broadening, quasi-resonance, phase modulation.*

1. Introduction

Practical applications and theoretical study of the double resonance have long attracted attention of researchers [1]. The pulsed regime of this phenomenon for exciting pulses of duration substantially longer than the irreversible relaxation time of quantum transitions was extensively investigated in papers devoted to the study of electromagnetically induced transparency [2, 3]. In this paper, the regime appearing upon excitation by pulses of duration much shorter than the relaxation time, so that the effect of relaxation processes is in fact excluded, is called the transient double-resonance regime. The theory of the linear stage of transient double resonance, in the case when the influence of a weak field on a high-power field can be neglected, predicted the possibility of the exponential weak-pulse gain [4 – 8]. The possibility of formation of simultons and a strong transfer of the high-power pulse energy to that of a weak pulse were strictly substantiated in papers [5, 9, 10]. The transient double resonance under conditions when the two interacting pulses satisfy the adiabaticity criterion was theoretically investigated in paper [11].

The analytic results of the theory of the nonlinear stage of transient double resonance obtained at present are mainly related to spectrally homogeneous media. In real media, for example, rarefied gases, spectral transitions are inhomogeneously broadened. The numerical study of the transient double resonance taking into account the spectral inhomogeneity of a medium for a scheme with a common intermediate level and equidistant energy spectrum was performed in paper [12].

The numerical simulation of the transient double resonance for a scheme with a common upper level (the Λ scheme) in a spectrally inhomogeneous medium in the case of an exact resonance of each of the interacting pulses with the corresponding quantum transition was performed in paper [13]. The aim of our paper is to simulate numerically this process in the case of quasi-resonance, i.e, in the presence of small frequency detunings of the pulses from the central frequencies of quantum transitions. We will consider only the situations when the inhomogeneous width of a quantum transition with a high frequency considerably exceeds the spectral widths of the interacting pulses on the input surface of a resonance medium. This allows us to interpret the results by using some analytic conclusions obtained in the study [6] of the nonlinear regime of the double resonance of this type. By considering only the coherent aspects of the interaction of radiation with a medium, we neglect irreversible relaxation processes.

2. Formulation of the boundary problem

To take the inhomogeneous broadening into account, we consider rarefied gases in which resonance transitions are broadened due to the Doppler effect. We will simulate such a medium by an ensemble of three-level quantum objects, which we will call below atoms, with non-degenerate levels, which are numerated in the order of energy increasing by the numbers 1, 2, and 3. The quantities p_{13} and p_{23} are the z components of the electric dipole transitions 1 – 3 and 2 – 3, ω_{310} and ω_{320} are the frequencies of these transitions for atoms at rest, respectively (Fig. 1). The 1 – 2 transition is assumed forbidden in the electric dipole approximation. We assume that radiation incident on the medium propagates along the x axis, and V_x is the velocity of the thermal motion of an atom along this axis. Due to the Doppler effect, the frequency ω_{3i} ($i = 1, 2$) of the $3 - i$ transition of a moving atom is described by the expression $\omega_{3i} - \omega_{3i0} =$

A.E. Dmitriev, O.M. Parshkov Saratov State Technical University, ul. Politekhnicheskaya 77, 410054 Saratov, Russia;
e-mail: tech@mail.saratov.ru; web-site: http: //www.sstu.runnet.ru

Received 20 December 2004; revision received 5 April 2005
Kvantovaya Elektronika **35** (8) 749 – 755 (2005)
Translated by M.N. Sapozhnikov

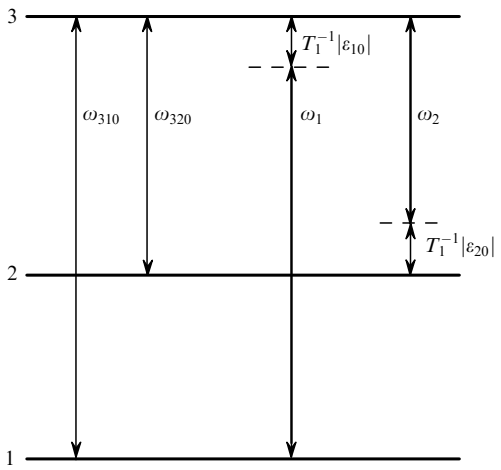

Figure 1. Diagram of quantum transitions (ω_1 and ω_2 are the pump and signal radiation frequencies, respectively).

$(\omega_{3i0}/c)V_x$. Because of the one-to-one correspondence between V_x and ω_{31}, we can use the frequency ω_{31} as the main parameter characterising the moving atom. The frequency ω_{32} is a linear function of the frequency ω_{31}

$$\omega_{32} = \omega_{320} + \frac{\omega_{320}}{\omega_{310}}(\omega_{31} - \omega_{310}). \tag{1}$$

Due to a random thermal motion of gas atoms, the frequency ω_{31} is a random quantity with the probability density specified by a Gaussian [14]. Let us denote by T_1 the inverse half-width of this function at the e^{-1} level.

We represent the electric field strength $\boldsymbol{E}$ of radiation as a sum of two quasi-harmonics polarised along the z axis and propagating along the x axis:

$$\boldsymbol{E} = \boldsymbol{k}\mu_1 E_1 \cos(k_1 x - \omega_1 t + \phi_1) + \boldsymbol{k}\mu_2 E_2 \cos(k_2 x - \omega_2 t + \phi_2), \tag{2}$$

where $\boldsymbol{k}$ the unit vector along the z axis; ω_i and $k_i = \omega_i/c$ are the carrier frequencies and wave numbers of quasi-harmonics at the input ($x = 0$) to the resonance medium; $\mu_i = \hbar/(T_1|p_{i3}|)$; $E_i = E_i(x,t)$ and $\phi_i = \phi_i(x,t)$ are the real amplitudes and phase shifts of the quasi-harmonic with the subscript i. We will call quasi-harmonics with frequencies ω_1 and ω_2 ($\omega_1 > \omega_2$) the pump and signal radiation, respectively (Fig. 1).

We will analyse the system of equations written in the slowly varying envelope approximation [15, 16] for the complex amplitudes $a_i = E_i \exp(\mathrm{i}\phi_i)$ of the interacting pulses and the amplitudes σ_{jk} ($j,k = 1, 2, 3$) of the elements of the density matrix:

$$\frac{\partial a_1}{\partial s} = \frac{\mathrm{i}}{\sqrt{\pi}}\int_{-\infty}^{+\infty} \sigma_{31} \exp\left[-(\varepsilon_1 - \varepsilon_{10})^2\right] \mathrm{d}\varepsilon_1,$$

$$\frac{\partial a_2}{\partial s} = \frac{\mathrm{i}}{\sqrt{\pi}}\alpha\int_{-\infty}^{+\infty} \sigma_{32} \exp\left[-(\varepsilon_1 - \varepsilon_{10})^2\right] \mathrm{d}\varepsilon_1,$$

$$\frac{\partial \sigma_{31}}{\partial w} + \mathrm{i}\varepsilon_1\sigma_{31} = \mathrm{i}a_1(\sigma_{11} - \sigma_{33}) + \mathrm{i}a_2\sigma_{21},$$

$$\frac{\partial \sigma_{32}}{\partial w} + \mathrm{i}\varepsilon_2\sigma_{32} = \mathrm{i}a_2(\sigma_{22} - \sigma_{33}) + \mathrm{i}a_1\sigma_{12},$$

$$\frac{\partial \sigma_{21}}{\partial w} + \mathrm{i}(\varepsilon_1 - \varepsilon_2)\sigma_{21} = \frac{\mathrm{i}}{4}a_2^*\sigma_{31} - \frac{\mathrm{i}}{4}a_1\sigma_{23}, \tag{3}$$

$$\frac{\partial \sigma_{11}}{\partial w} = \frac{1}{2}\mathrm{Im}(a_1\sigma_{31}^*), \quad \frac{\partial \sigma_{22}}{\partial w} = \frac{1}{2}\mathrm{Im}(a_2\sigma_{32}^*),$$

$$\frac{\partial \sigma_{33}}{\partial w} = -\frac{1}{2}\mathrm{Im}(a_1\sigma_{31}^*) - \frac{1}{2}\mathrm{Im}(a_2\sigma_{32}^*),$$

$$\varepsilon_2 = \varepsilon_{20} + \beta(\varepsilon_1 - \varepsilon_{10}). \tag{4}$$

Here,

$$s = \frac{x}{x_1} \quad \text{и} \quad w = \frac{1}{T_1}\left(t - \frac{x}{c}\right)$$

are the dimensionless independent variables; $x_1 = c\hbar/(2\pi\omega_1 \times |p_{13}|^2 N T_1)$ is the distance multiplied by $\sqrt{\pi}$ at which the amplitude of weak radiation at the frequency ω_{310} decreases by a factor of e due to the inhomogeneous broadening, i.e., due to the interference of radiation of atomic dipoles with frequencies distributed within the inhomogeneous $1-3$ transition line [17]; N is the concentration of atoms; α and β are the dimensionless parameters determined by the relations

$$\alpha = \frac{\omega_2|p_{23}|^2}{\omega_1|p_{13}|^2}, \qquad \beta = \frac{\omega_{320}}{\omega_{310}}. \tag{5}$$

The parameter α is the ratio of the oscillator strengths for the $2-3$ and $1-3$ transitions. The dimensionless frequency detunings from the resonance are specified by the expressions

$$\varepsilon_i = T_1(\omega_{3i} - \omega_i), \quad \varepsilon_{i0} = T_1(\omega_{3i0} - \omega_i), \tag{6}$$

i.e., the quantity ε_i characterises the deviation of the radiation frequency $i-3$ of a moving atom from the resonance frequency ω_i, whereas the quantity ε_{i0} determines this deviation for an atom at rest (Fig. 1).

System (3) is supplemented with the boundary ($s = 0$) and initial ($w = 0$) conditions:

$$a_i(s = 0, w) = a_{i0}(w), \qquad w \geqslant 0,$$

$$\sigma_{jk}(s, w = 0) = 0, \qquad j \neq k, \quad s \geqslant 0, \tag{7}$$

$$\sigma_{11}(s, w = 0) = 1, \quad \sigma_{jj}(s, w = 0) = 0, \quad j = 2, 3, \; s \geqslant 0.$$

Here, $a_{i0}(w)$ are the complex envelopes of the pump and signal pulses at the input surface $s = 0$ of the resonance medium. The conditions imposed by expressions (7) on the amplitudes σ_{jk} correspond to the case of an initially unexcited medium in which all the atoms occupy the ground level.

The boundary problem (3), (7) was solved numerically by using the program based on the predictor–corrector

scheme by controlling the calculation accuracy with the help of the Runge rule [18, 19] and verifying the relation $\sigma_{11} + \sigma_{22} + \sigma_{33} = 1$. When the condition $a_{20}(w) = 0$ ($w \geqslant 0$) is fulfilled, this boundary problem coincides with the boundary problem describing self-induced transparency [17, 20]. The use of this program for simulating self-induced transparency has demonstrated good agreement with the known analytic results of the theory of this phenomenon and provided an accurate description of a number of experiments [21, 22].

3. Representation of calculation results

We represented the results of calculations in the form of dependence of the real envelopes $E_i(w) = |a_i(s = \text{const}, w)|$ and phase shifts $\phi_i(w) = \arg a_i(s = \text{const}, w)$ of the momentum with the frequency ω_i for a fixed s ($-\pi < \phi_i(w) \leqslant \pi$). The quantities $E_{mi}(s)$ and $\Theta_i(s)$ are the maximum values of the real envelopes and the area under them at the distance s from the input surface under the condition that the envelopes of pump and signal pulses are measured in units of μ_1^{-1} and the pulse full width at half-maximum τ is measured in the time units w.

The frequency characteristic of the signal pulse is described by the deviation $\tilde{\varepsilon}_{20} = T_1(\omega_{320} - \tilde{\omega}_2)$ of the instant frequency $\tilde{\omega}_2$ of the pulse from the central frequency of the 2–3 transition measured in units of T_1^{-1}. It is easy to show that $\tilde{\varepsilon}_{20} = \varepsilon_{20} + \partial\phi_2/\partial w$.

The spectral density $\Omega_2(\Delta)$ of signal radiation is defined as the square of the modulus of the Fourier transform of the function $2\boldsymbol{kE}_2/(\mu_2 T_1)$ at the frequency $\omega' = \omega_2 - \Delta/T_1$ for a fixed value of s. The quantity Δ introduced in this way is the detuning of the frequency ω' from the frequency ω_2 normalised to the width (at the e^{-1} level) of the Doppler contour of the 1–3 transition.

4. Results of calculations

We assumed in calculations that $\alpha = 2.25$ and $\beta = 0.91$. Such values of α and β are realised, for example, if the $5P_{1/2}$, $5P_{3/2}$, and $6S_{1/2}$ levels of the indium atom are used as levels 1, 2, and 3 [6]. It was shown in [6] that for large inhomogeneous broadening, the condition $\alpha > 0.25(2 - \beta)^2$, which is satisfied in this case, means the possibility of the exponential gain of a weak signal pulse in the field of a high-power pump pulse. The function $a_{10}(w)$ describing the real envelope of the input pump pulse was written in the form

$$a_{10}(w) = 0.3 \operatorname{sech} \frac{w - 40}{5}, \tag{8}$$

which corresponds to a pulse with $\Theta_1(0) = 1.5\pi$. For this pulse, $\tau = 13.2$, and therefore the width of its spectrum is considerably smaller than the Doppler width of the 1–3 transition. (For the above-mentioned transition in indium, $T_1 = 160$ ps at temperature 1120 K [6], and the pulse duration (8) was approximately 2 ns.) The 2π pulses appearing in calculations were identified by comparing their characteristics (the pulse area, the ratio of the pulse amplitude to its duration, the propagation velocity) with those predicted by the analytic theory of self-induced transparency [23]. A pulse was considered to be the 2π pulse if the discrepancy between the corresponding characteristics did not exceed 2 %.

4.1 Long weak input signal

We assume that the envelope of the input pump pulse is specified in form (8), and $\varepsilon_{10} = 1.0$, $\varepsilon_{20} = -1.0$, and $a_{20}(w) = 10^{-10}$ in (7). This value of $a_{20}(w)$ was used when the input signal pulse was much weaker and longer than the input pump pulse. Figure 2 shows the dependences of $E_{mi}(s)$ and $\Theta_i(s)$. The plateau of curve $\Theta_1(s)$ in Fig. 2b corresponding to $\Theta_1 = 6.28$ suggests that the pump pulse at distances $s = 5 - 20$ is a 2π pulse. Its real envelope and phase shift are presented in Fig. 3a. This 2π pulse has duration $\tau = 26.63$ and has no phase modulation ($\partial\phi_1/\partial w = 0$ in the pulse region). For s close to 20, the 2π pulse is rapidly destroyed, by imparting its energy to the signal pulse, which also rapidly increases, as shown by curves $E_{m2}(s)$ and $\Theta_2(s)$ in Fig. 2. These curves also show that the signal amplification ceases for $s > 25$, the maximum value of the envelope of the signal pulse $E_{m2}(s)$ at these distances exceeding somewhat that of the input pump pulse. The real envelope of the signal pulse and its phase shift for $s = 50$ are presented in Fig. 3b. (The discrepancy between the maximum values of the signal pulse envelopes in Figs 3b and 2a for $s = 50$ are explained by the fact that the maximum value of the signal pulse envelope in Fig. 2a, as that of the pump pulse, is measured in units of μ_1^{-1}, while in Fig. 3a it is measured in units of μ_2^{-1}.) Oscillations of the phase shift demonstrate the shift of the instant frequency of the signal pulse. Our analysis gives the value $\tilde{\varepsilon}_{20} = 0.917$.

As shown in [6], the carrier frequency $\tilde{\omega}_2$ at the linear stage of the transient double resonance shifts to the value at which the condition

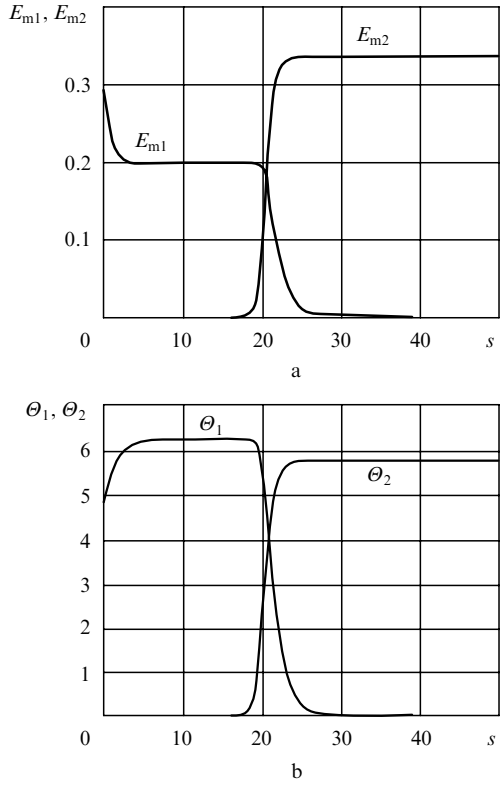

Figure 2. Dependences of the maximum values of the pump- and signal-pulse envelopes E_{m1} and E_{m2}, respectively, (a) and areas Θ_1 and Θ_2 under these envelopes (b) on s for a long weak input signal pulse.

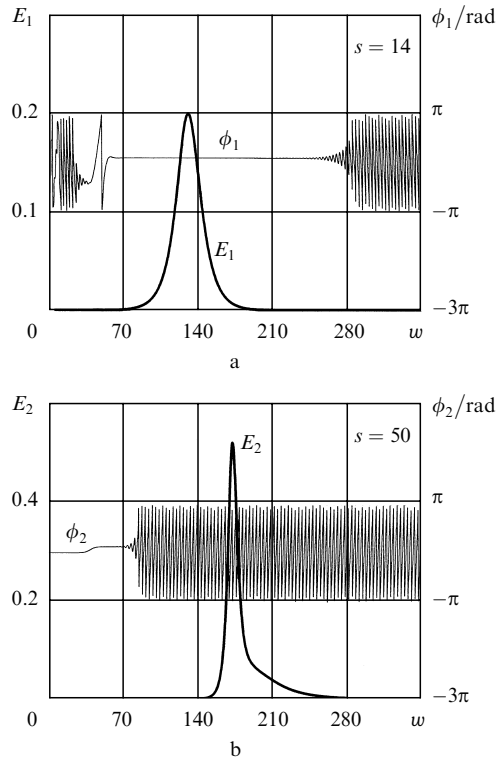

Figure 3. Pump-pulse envelope E_1 and its phase shift ϕ_1 for $s = 14$ (a) and the signal-pulse envelope E_2 and its phase shift ϕ_2 for $s = 50$ (b) for a long weak input signal pulse.

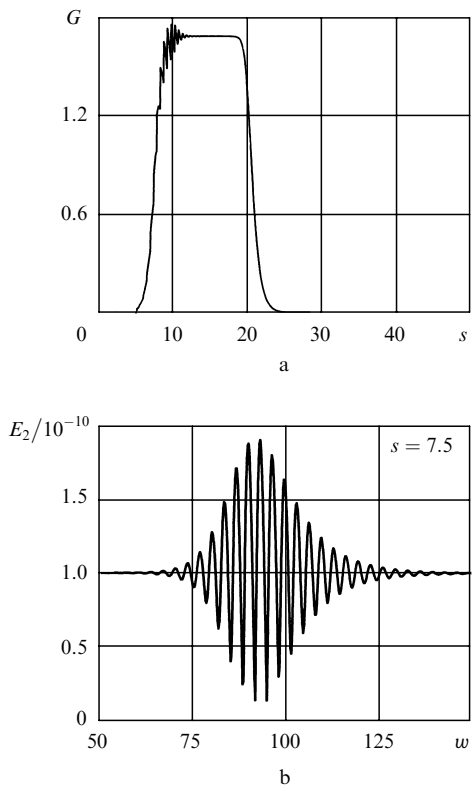

Figure 4. Dependence of the signal-pulse gain G on s (a) and the envelope of this pulse E_2 for $s = 7.5$ (b) for a long weak input signal.

$$\tilde{\varepsilon}_{20} = \beta\varepsilon_{20} \tag{9}$$

is fulfilled. According to (9), for the above values of β and ε_{10}, we have $\tilde{\varepsilon}_{20} = 0.91$. Such a good agreement of this value of $\tilde{\varepsilon}_{20}$ with the value presented above means that the shift of the carrier frequency of the signal pulse appearing at the linear stage of the double resonance is preserved almost invariable at a substantially nonlinear stage of this process. Our calculations showed that when $\Theta_1(0) > \pi$, the shift of the frequency $\tilde{\omega}_2$ is independent of the pump and signal fields, thus being substantially different from the frequency shift caused by the dynamic Stark effect, which is quadratic in the field strength amplitude [16].

Figure 4a presents the dependence of the local gain G of the signal pulse on s, which is described by the expression $G = \partial(\ln E_{m2})/\partial s$. A constant value of $G = 1.7$ for $s = 13 - 20$ means that the signal increases exponentially at such distances. The value of G is 1.7, whereas the linear theory [6] gives $G = 1.3$ in this case. Figure 4b shows the signal pulse envelope at the initial amplification stage. Oscillations in Fig. 4b, which we call below the interference beats, are predicted by the linear theory [6] and are caused by the interference of the input signal radiation and the signal pulse appearing at the shifted frequency.

4.2 Equal durations of the input signal and pump pulses

Let us assume that the pump pulse envelope is described by expression (8) and $\varepsilon_{10} = 1.5$. We represent the input signal amplitude in the form

$$a_{20}(w) = 0.3\mathrm{sech}\frac{w - 40}{5}, \quad \varepsilon_{20} = -1.5. \tag{10}$$

In this case, $\Theta_2(0) = 3.0$ and condition (9) for $s = 0$ is not fulfilled. Figure 5 presents the dependences $E_{mi}(s)$ and $\Theta_i(s)$. The form of the dependences $E_{m1}(s)$ and $\Theta_1(s)$ and their detailed analysis suggest that the pump pulse for $s = 10 - 25$ is a 2π pulse of the same duration as in the previous calculation. For $s > 25$, the 2π pulse is destroyed. The dependences $E_{m2}(s)$ and $\Theta_2(s)$ have a plateau for small s and rapidly increase up to a limit for $s > 25$.

Figure 6 presents the envelopes and phase shifts of the signal for $s = 28$ and 44. One can see that signal radiation consists of two pulses. One of them [pulse (*1*) in Fig. 6], which we call the leading pulse, represents the input signal pulse propagating in the medium almost without interaction with the pump pulse. Another pulse, which we call the delayed pulse [pulse (*2*) in Fig. 6], appears at the rear edge of pulse (*1*), and receiving its energy from pump radiation, increases with increasing s. Pulse (*2*), as follows from our analysis, is modulated in phase so that condition (9) is fulfilled (with an accuracy less than 2 %) beginning from the linear stage of the appearance of this pulse. Note that interference beats occur at this stage.

Figure 7 shows the spectrum of signal radiation for $s = 44$. Spectral line (*1*) in this figure is the spectrum of the leading signal pulse, while spectral line (*2*) is the spectrum of the delayed signal pulse. The position of line (*2*) well agrees with condition (9). Indeed, in the case of symmetric bell-shaped envelopes, the central frequency of the pulse spectrum is close to its carrier frequency. This means that $\tilde{\varepsilon}_{20} \approx \varepsilon_{20} + \Delta_0$, where Δ_0 is the spectral line position on the Δ axis. For line (*2*) in Fig. 7, we have $\Delta_0 = 2.88$, so that $\tilde{\varepsilon}_{20} = 1.38$. On the other hand, $\beta\varepsilon_{10} = 1.37$, which is close to the value of $\tilde{\varepsilon}_{20}$.

Let us present the results of calculation for the case

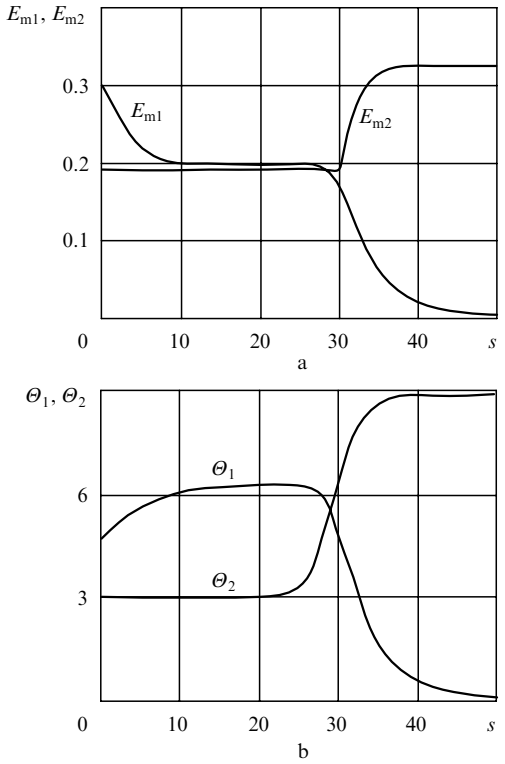

Figure 5. Dependences of the maximum values of the pump- and signal-pulse envelopes E_{m1} and E_{m2}, respectively, (a) and areas Θ_1 and Θ_2 under these envelopes (b) on s for a short input signal when condition (9) is not fulfilled.

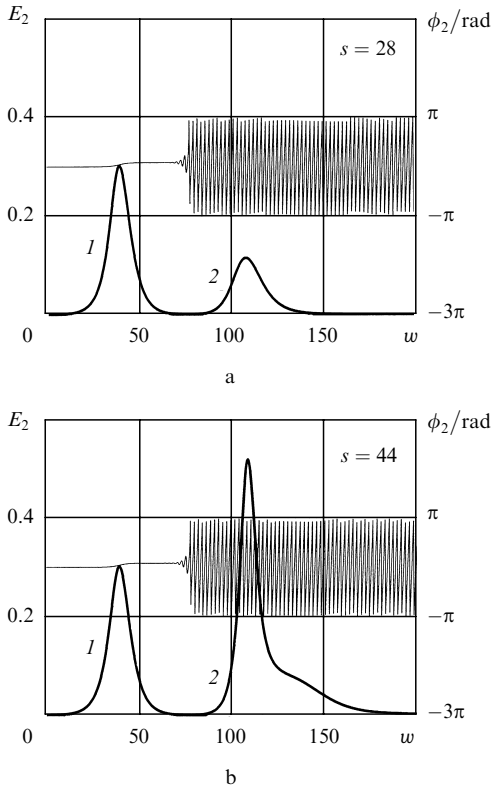

Figure 6. Signal-pulse envelopes E_2 (thick curves) and phase shifts ϕ_2 (thin curves) for $s = 28$ (a) and 44 (b) and a short input signal when condition (9) is not fulfilled. Curves (*1*) and (*2*) are the leading and delayed signal radiation pulses.

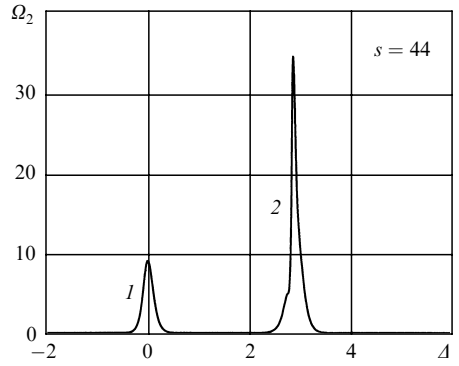

Figure 7. Spectra of the leading (*1*) and delayed (*2*) signal radiation for $s = 44$ and a short input signal when condition (9) is not fulfilled.

$\varepsilon_{20} = 1.4$, which well corresponds to the fulfilment of equality (9). All the other parameters and boundary conditions remain the same as in the previous calculation. The dependences $E_{mi}(s)$ and $\Theta_i(s)$ are presented in Fig. 8. The shape of curves $E_{m1}(s)$ and $\Theta_1(s)$ show that the pump pulse does not transform to the 2π pulse but monotonically decreases with increasing s. The dependences $E_{m2}(s)$ and $\Theta_2(s)$ demonstrate a monotonic saturable gain of the signal pulse. Figure 9a shows the envelope and phase shift of signal radiation for $s = 20$. One can see that the total energy of the signal is contained in one pulse, which virtually has no phase modulation ($|\partial\phi_2/\partial w| \approx 0.01$ instead of 2.9 in the previous calculation). The spectrum of this pulse, as follows from Fig. 9b, contains only one spectral line.

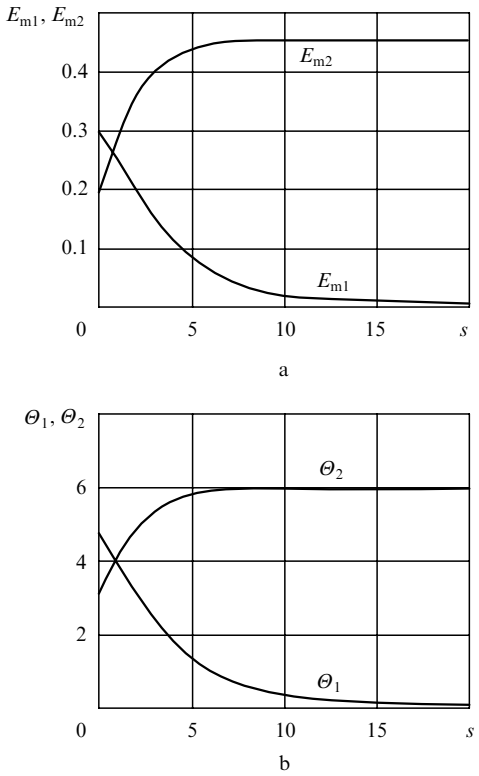

Figure 8. Dependences of the maximum values of the pump- and signal-pulse envelopes E_{m1} and E_{m2}, respectively, (a) and areas Θ_1 and Θ_2 under these envelopes (b) on s for a short input signal when condition (9) is fulfilled.

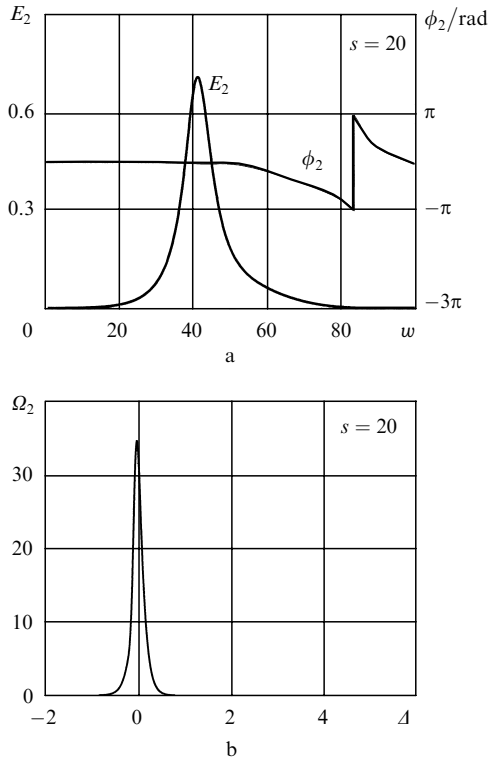

Figure 9. Real envelope E_2 and the phase shift (a) and the spectral density Ω_2 of the signal pulse (b) for $s = 20$ and a short input signal when condition (9) is fulfilled.

The results of three calculations considered above and some calculations for different values of parameters of the resonance medium and input pulses can be simply explained. The width of the Doppler line of the $1-3$ transition greatly exceeds the spectral width of the input pump pulse. Therefore, the pump pulse excites efficiently not all but only the moving atoms, which we will call active atoms, for which the resonance condition $\omega_{31} = \omega_1$ is well satisfied. The perturbation of the active atoms is localised in the pump pulse region and moves with the pump pulse at the velocity that is noticeably lower than the speed of light c in vacuum because of the inertia of the polarisation response of the medium. By using expression (1), we can easily show that for active atoms,

$$\varepsilon_2 \approx -\beta\varepsilon_{10} + \varepsilon_{20}. \tag{11}$$

For the opposite signs of detunings ε_{10} and ε_{20}, their sufficiently large absolute values and the value of β close to unity, the fulfilment of condition (11) means a substantial deviation of the signal beam frequency from the resonance with the $2-3$ transition in active atoms. As a result, the input signal pulse does not interact in fact with the medium and, propagating at the velocity c, overtakes the pump pulse by forming the leading pulse. The interaction of the rear edge of the leading pulse with the pump pulse leads to the appearance of a delayed signal pulse. Because the polarisation response is transient, the carrier frequency of this pulse is 'tuned' to resonance with the $2-3$ transition in active atoms, which provides the efficient energy transfer from the pump to signal pulse.

When condition (9) is fulfilled, it follows from (11) that $\varepsilon_2 = 0$, i.e., the $2-3$ transition in active atoms proves to be resonant with the input signal pulse. The efficient pump energy transfer to the rear edge of the signal pulse is manifested in this case as the 'locking' of the signal pulse by the pump pulse. As a result, signal radiation has a single-pulse structure.

5. Conclusions

The numerical simulation of the transient double resonance in the case of a large inhomogeneous broadening of quantum transitions performed in the paper well reproduces the main results of the analytic theory linear in the signal field [6]. In the case of approximately equal durations of the pump and signal pulses, their interaction, when condition (9) is fulfilled, results in a single-pulse structure of the signal field. When condition (9) is strongly violated, the signal field has a two-pulse structure. This is explained by the specific interaction of the pulses with Doppler-broadened quantum transitions in an ensemble of three-level atoms. We are not aware of any experimental observations of the above-described effects. Note in this connection that the signal frequency pulling to the frequency satisfying condition (9) can be used (if the pump pulse frequency is stable) to stabilise the signal radiation frequency. By varying the detunings of the input signal and pump pulses from the resonance, one can produce pairs of the leading and delayed signal pulses with a controlled repetition period.

As objects for experiments on the observation of effects described in the paper, except the above-mentioned transitions in indium atoms, it is possible, for example, to study quantum transitions in the ^{208}Pb vapour, which were investigated in experiments on electromagnetically induced transparency [24]. In this case, the duration of the interacting pulses should be shorter than in paper [24]. To provide the correspondence between our model and experiment (large inhomogeneous broadening and the absence of relaxation processes), the duration of both interacting pulses should be approximately 2 ns.

References

1. Shimoda K., in *Laser Spectroscopy of Atoms and Molecules*, Ed. by Walther H. (New York: Springer-Verlag, 1976; Moscow: Mir, 1979).
2. Agap'ev B.D., Gornyi M.B., Matisov B.G., Rozhdestvenskii Yu.V. *Usp. Fiz. Nauk*, **163**, 1 (1993); Popov A.K. *Izv. Ross. Akad. Nauk, Ser. Fiz.*, **60**, 99 (1996).
3. Harris S.E. *Physics Today*, (7), 36 (1997); Marangos J.P. *J. Mod. Phys.*, **45**, 472 (1998).
4. Medvedev B.A., Parshkov O.M., Gorshenin V.A., Dmitriev A.E. *Zh. Eksp. Teor. Fiz.*, **67**, 70 (1974).
5. Bol'shov L.A., Elkin N.N., Likhanskii V.V., Persiantsev M.I. *Pis'ma Zh. Eksp. Teor. Fiz.*, **39**, 360 (1984); *Opt. Commun.*, **51**, 201 (1984); *Zh. Eksp. Teor. Fiz.*, **88**, 47 (1985).
6. Dmitriev A.E., Parshkov O.M. *Kvantovaya Elektron.*, **14**, 498 (1987) [*Sov. J. Quantum Electron.*, **17**, 309 (1987)].
7. Dmitriev A.E., Parshkov O.M. *Kvantovaya Elektron.*, **13**, 712 (1986) [*Sov. J. Quantum Electron.*, **16**, 464 (1986)].
8. Dmitriev A.E., Parshkov O.M. *Kvantovaya Elektron.*, **20**, 447 (1993) [*Quantum Electron.*, **23**, 385 (1993)].
9. Bol'shov L.A., Likhanskii V.V., Persiantsev M.I. *Zh. Eksp. Teor. Fiz.*, **84**, 903 (1983).
10. Maimistov A.I. *Kvantovaya Elektron.*, **11**, 567 (1984) [*Sov. J. Quantum Electron.*, **14**, 385 (1984)].

11. Arkhipkin V.G., Timofeev I.V. *Kvantovaya Elektron.*, **30**, 180 (2000) [*Quantum Electron.*, **30**, 180 (2000)].
12. Gruev D.I. *Kvantovaya Elektron.*, **6**, 1422 (1979) [*Sov. J. Quantum Electron.*, **9**, 834 (1979)].
13. Vershinin A.L., Dmitriev A.E., Parshkov O.M., Pisnoi A.L. *Kvantovaya Elektron.*, **32**, 33 (2002) [*Quantum Electron.*, **32**, 33 (2002)].
14. Letokhov V.S., Chebotaev V.P. *Nelineuinaya lazernaya spektroskopiya vysokogo razresheniya* (High-resolution Nonlinear Laser Spectroscopy) (Moscow: Nauka, 1990).
15. Akhmanov S.A., Khokhlov R.V. *Problemy nelineinoi optiki: Elektromagnitnye volny v nelineinykh dispergiruyushchikh sredakh* (Problems of Nonlinear Optics: Electromagnetic Waves in Nonlinear Dispersion Media) (Moscow: Izd. Akad. Nauk SSSR, 1965).
16. Butylkin V.S., Kaplan A.E., Khronopulo Yu.G., Yakubovich E.I. *Rezonansnye vzaimodeistviya sveta s veshchestvom* (Resonance Interactions of Light with Matter) (Moscow: Nauka, 1977).
17. McCall S.L., Hahn E.L. *Phys. Rev.*, **183**, 457 (1969).
18. Bakhvalov N.S., Zhidkov N.P., Kobel'kov G.M. *Chislennye metody* (Numerical Methods) (Moscow: Fizmatlit, 2002).
19. Krylov V.I., Bobkov V.V., Monastyrskii P.I. *Vychislitel'nye metody* (Computing Methods) (Moscow: Nauka, 1977).
20. Lamb G.L. Jr. *Rev. Mod. Phys.*, **43**, 99 (1971).
21. Dmitriev A.E., Parshkov O.M. *Kvantovaya Elektron.*, **33**, 993 (2003) [*Quantum Electron.*, **33**, 993 (2003)].
22. Dmitriev A.E., Parshkov O.M. *Kvantovaya Elektron.*, **34**, 652 (2004) [*Quantum Electron.*, **34**, 652 (2004)].
23. Lamb G.L. Jr. *Phys. Rev. Lett.*, **31**, 196 (1973).
24. Kasapi A., Maneesh Jain, Yin G.Y., Harris S.E. *Phys. Rev. Lett.*, **74**, 2447 (1995).